Ultrasound in Med. & Biol., Vol. 42, No. 5, pp. 1058–1065, 2016

0301-5629/$ - see front matter

http://dx.doi.org/10.1016/j.ultrasmedbio.2015.08.021

● *Original Contribution*

EFFICACY OF ABLATION THERAPY FOR SECONDARY HYPERPARATHYROIDISM BY ULTRASOUND GUIDED PERCUTANEOUS THERMOABLATION

JUNFENG ZHAO, LINXUE QIAN, YUAN ZU, YING WEI, and XIANGDONG HU
Department of Ultrasound, Beijing Friendship Hospital Affiliated to Capital Medical University, Beijing, China

(*Received* 23 *June* 2014; *revised* 20 *August* 2015; *in final form* 31 *August* 2015)

Abstract—The objective of this study was to explore the value of ultrasound-guided percutaneous microwave thermoablation to treat secondary hyperparathyroidism (SHPT). One hundred and thirty-eight parathyroid glands from 56 patients with SHPT were ablated in this study. All the parathyroid glands were evaluated by real-time contrast-enhanced ultrasound before, during and after ablation. Changes in serum parathyroid hormone (sPTH) levels were measured before treatment and at 1 h, 1 wk, 1 mo and 6 mo after thermoablation treatment. All 56 cases had a 1-mo follow-up, and 34 cases had a 6-mo follow-up. The sPTH level of the 54 cases 1 mo after ablation was significantly lower than that before ($p < 0.05$). In the 34 cases that had a 6-mo follow-up, the sPTH levels were also significantly lower at 6 mo after ablation than before ($p < 0.05$). Bone pain in patients improved post-operatively ($p < 0.05$), but itchiness and insomnia did not improve ($p > 0.05$). Ultrasound-guided percutaneous microwave thermoablation is a feasible and effective non-surgical alternative treatment for SHPT patients. (E-mail: qianlinxue2002@163.com) © **2016 Published by Elsevier Inc. on behalf of World Federation for Ultrasound in Medicine & Biology.**

Key Words: **Secondary hyperparathyroidism, Serum parathyroid hormone, Thermal ablation, Ultrasound.**

INTRODUCTION

Chronic kidney disease (CKD) is a major chronic disease with a devastating effect on human health. CKD has a morbidity of 10%, as many patients will progress to chronic renal failure (CRF). About 26.3% of CKD patients have combined secondary hyperparathyroidism (SHPT), which is the most common serious complication of CRF (Douthat et al. 2003; Young et al. 2004). Serum parathyroid hormone (sPTH) is the main hormone that regulates serum calcium and phosphorous levels. Low serum calcium and high serum phosphorus can cause mental abnormalities, muscle spasms and even lead to respiratory or cardiac arrest (Moe et al. 2006; Zhang et al. 2013b). Among the symptoms, bone pain, itching and insomnia are typical, which seriously affect the life quality of patients (Yao et al. 2009). Traditional treatment strategies for SHPT include drug treatment and parathyroid surgery. For refractory SHPT, drug therapy is ineffective, but surgical treatment is invasive and traumatic. Furthermore, many patients do not tolerate surgical treatment. As a result, an effective, minimally invasive therapeutic strategy is needed for the treatment of SHPT.

Current guidelines on refractory SHPT incorporate complicated treatment options that are difficult to use clinically and have very low drug control effect (Bolasco 2011; Morrone et al. 2011; Panichi et al. 2010) and poor treatment efficacy. When patients with SHPT develop hyperplasia that is visible on imaging, but the hyperplastic tissue is small or fewer than four visible hyperplastic parathyroids are found, surgical removal of the parathyroid might not be complete and a secondary surgery might be needed. Because growth control of the parathyroid could be damaged in late nodular hyperplasia of parathyroid with CRF, the parathyroid might result in local invasive growths (Olson and Leight 2002), and this is the cause of recurrent symptoms after treatment of secondary hyperparathyroidism. The 1-y recurrence rate of gland resection can be as high as 30% (Olson and Leight 2002) or patients can be reluctant to undergo surgery.

Address correspondence to: Linxue Qian, Department of Ultrasound, Beijing Friendship Hospital Affiliated to Capital Medical University, Beijing 100050, China. E-mail: qianlinxue2002@163.com

Conflict of interest: This paper has not been published elsewhere in whole or in part. All authors have read and approved the content, and agree to submit for consideration for publication in the journal. There are no any ethical/legal conflicts involved in the article.

Ultrasound-guided interventions are an effective alternative (Lacobone 2006). Recent reports generally indicate ultrasound-guided percutaneous alcohol injection therapies (Chen et al. 2011; Douthat et al. 2011) for clinical applications have gradually been recognized. Ethanol injection therapy is more commonly used as a minimally invasive treatment of SHPT, but incomplete ablation with a 1-y recurrence rate of 80% has limited its clinical application.

Recently, thermal ablation treatments have changed SHPT treatment. Microbubbles are generated by ablation and detectable by ultrasound imaging. It was reported that using radiofrequency can ablate tumors ≤5 cm and the tumor inactivation rate could be >90% (Lencioni et al. 2003; Lin et al. 2004; Shiina et al. 2005). Furthermore, differences in the efficacy and long-term survival rate after microwave ablation and radiofrequency ablation were not statistically significant (Lu et al. 2005; Shibata et al. 2002). Research on the 3-D ablation thermal field using finite elements has laid a solid theoretic and technical foundation for the clinical application of ablation technology (Liang et al. 2001; Tungjitkusolmun et al. 2002). The use of laser therapy and ultrasound-guided percutaneous radiofrequency tissue ablation of a solitary adenoma of the parathyroid gland have been described (Bennedbaek et al. 2001; Hänsler et al. 2002). Ultrasound-guided percutaneous microwave ablation of benign thyroid nodules was reported as a feasible technique (Feng et al. 2012), and microwave ablation to clinically treat SHPT should be feasible.

This study evaluated the use of ultrasound-guided percutaneous microwave thermoablation to treat SHPT.

MATERIALS AND METHODS

This study was approved by the Capital Medical University Ethics Committee and written informed consent was obtained from all patients before the study.

Participants

Fifty-six patients presenting with SHPT to the Department of Nephrology at Beijing Friendship Hospital from September 2012 to September 2013 were enrolled in this study. The patients included 26 males and 30 females with an age range of 29–82 y (55.02 ± 10.01). The average period of hemodialysis was 7.89 y with a range of 3.5 to 12 y; the average level of sPTH was 1256.4 pg/mL with a range of 638–2500 pg/mL. The average longitudinal diameter of nodules was 1.35 cm with a range of 0.5–3.5 cm.

Inclusion/exclusion criteria

Patients who were diagnosed with SHPT (sPTH >300 pg/mL) and the presence of parathyroid gland hyperplasia determined by ultrasound (Fig. 1a) and radionuclide imaging were included (Fig. 1b). Patients were

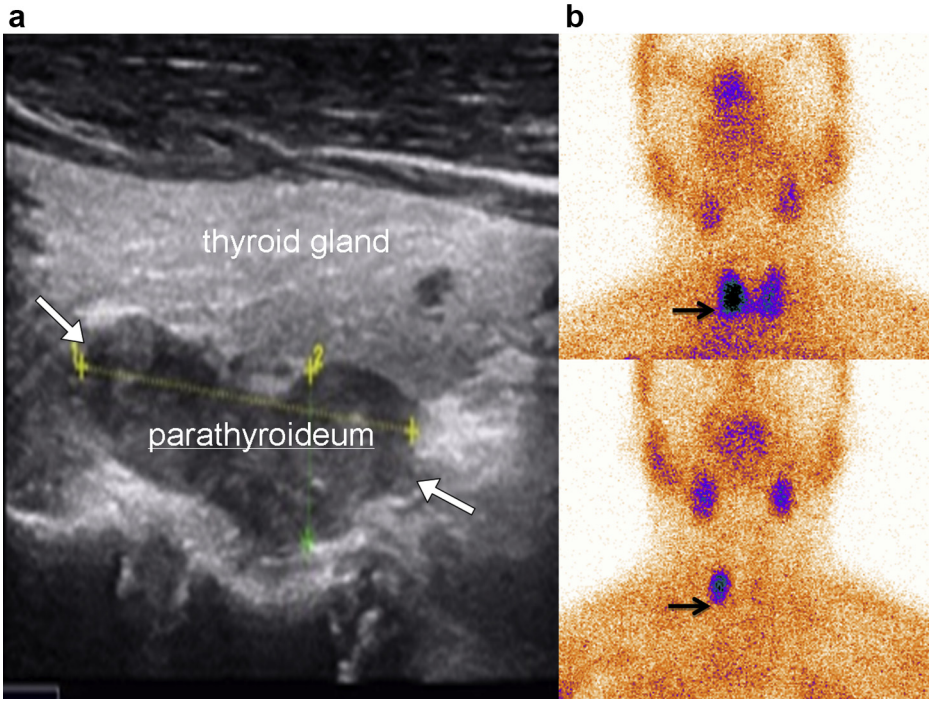

Fig. 1. A 54-y-old male with SHPT and CRF for 10 y. (a) B-mode ultrasound reveals a parathyroid hyperplasia of 28.0 × 8.5 mm (*arrow*). (b) A radionuclide image reveals the same parathyroid hyperplasia. SHPT = secondary hyperparathyroidism; CRF = chronic renal failure.

excluded if radionuclide imaging revealed an ectopic parathyroid hyperplasia that the microwave antenna pin or needle probe could not reach or if the parathyroid had been removed for autologous transplantation. Additionally, patients who had received kidney transplants; undergone chemotherapy; or who had other diseases such as coronary heart disease, tuberculosis or those that influence bone metabolism, serum calcium or serum phosphorous were also excluded. Patients taking glucocorticoids or patients with difficult parathyroid punctures that would inhibit complete ablation were also excluded.

Procedures

All procedures used a Phillips IU22 ultrasound imaging platform (Amsterdam, Netherlands). All patients were diagnosed using a L12-5 transducer of frequency 5–12 MHz. Microwave therapeutic equipment (KY-2000; Kangyou Medical, Nanjing, China) was used to administer microwave energy at a frequency of 2450 MHz. The microwave generator is capable of producing up to 100 W of power (30 W power was used in the study) with an antenna diameter of 2 mm, a total length of 100 mm and a transmit segment length of 5 mm. SonoVue (Bracco, Italy) was used as the ultrasound contrast agent; it is sulfur hexafluoride gas contained in a phospholipid shell.

Pre-operative procedures included collection of disease history focusing on history of kidney disease and dialysis, metabolic bone disease (measured on a pain rating scale ranging from 1 to 10 [Hensley and Courtney 2014]), insomnia (measured by the Athens insomnia scale that includes eight sleep factors with four levels within each [Bornivelli et al. 2008; Liu et al. 2014]) and itchy skin (measured by a visual analogue scale ranging from 1 to 10 [Keithi-Reddy et al. 2007]) symptoms. Laboratory tests of sPTH, serum calcium and phosphorous concentrations were also performed. Routine blood work and clotting tests were also verified to be normal before proceeding with the study. Parathyroid ultrasound (Fig. 1a), to measure the length and diameter of the parathyroid along the long axis in longitudinal sections and short axis on transverse sections and radionuclide imaging (^{99m}Tc-MIBI; Fig. 1b) were used to confirm the number, size and blood supply of parathyroid glands in every patient.

Before ablation, the parathyroid blood supply was confirmed with contrast-enhanced ultrasound (CEUS) (Fig. 4a) and the ablation pathway was decided. SonoVue (59 mg of lyophilized powder and 5 mL of 0.9% sodium chloride solution) was mixed according to manufacturer protocols. Patients' necks were hyperextended to expose the parathyroideum. Scanning was performed by one experienced sonographer, who was asked to evaluate the nodule location, size and Doppler flow signals. The standard view of CEUS was the section with the most abundant blood-flow signals within the lesion. The CEUS imaging mode was used, focus was positioned under the trailing edge of the lesion and the gain was adjusted to display only the boundaries of the lesion.

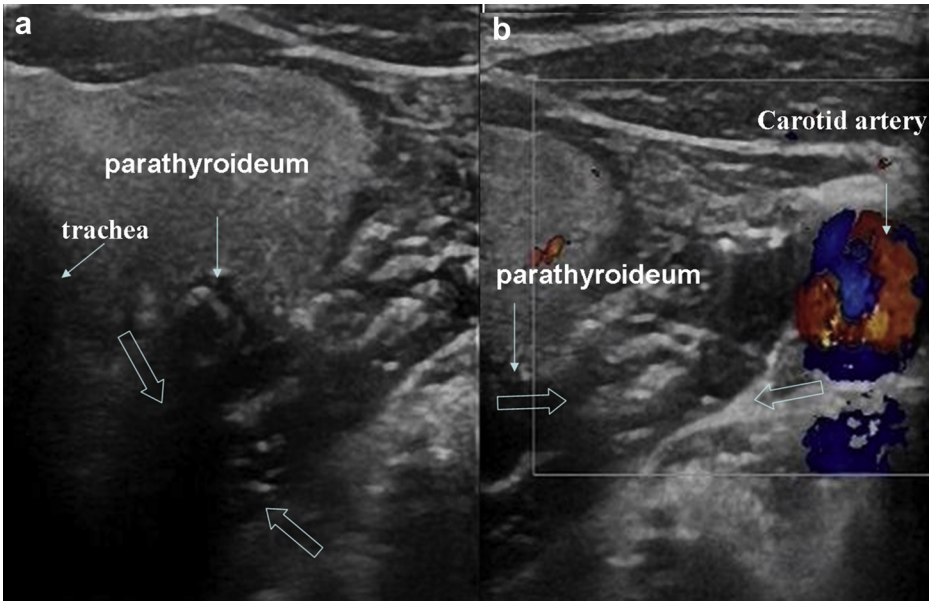

Fig. 2. A 49-y-old male with SHPT and CRF for 8 y. (a) Before ablation, a liquid isolation zone >1 cm wide was created between the parathyroid and the trachea and esophagus (*coarse arrow*). (b) Before ablation, a liquid isolation zone >1 cm wide was created between parathyroid and carotid artery (*coarse arrow*). SHPT 5 secondary hyperparathyroidism; CRF 5 chronic renal failure.

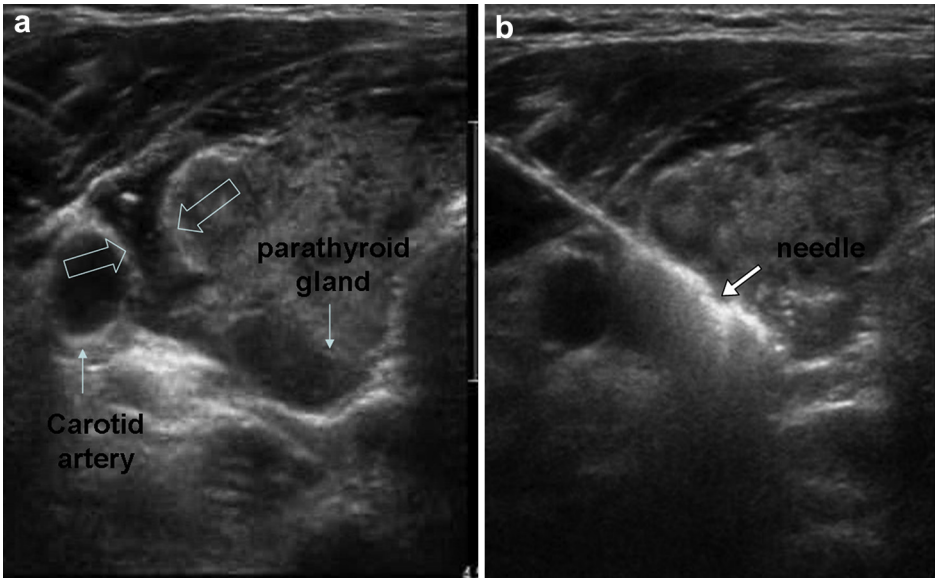

Fig. 3. A 54-y-old male with SHPT because of CRF for 10 y. (a) Before ablation, a liquid isolation zone was created between the parathyroid and adjacent structures. (b) B-mode ultrasound shows the antenna (*arrow*) placed in the nodule. SHPT = secondary hyperparathyroidism; CRF = chronic renal failure.

The transducer was turned on, and then 1.2 mL of SonoVue was injected into the ulnar vein, followed by injection of 5 mL of normal saline as a flush.

During the investigation, the position of the probe was moved around the nodule, and the patient was asked to avoid swallowing and breath holding. The quiet state and

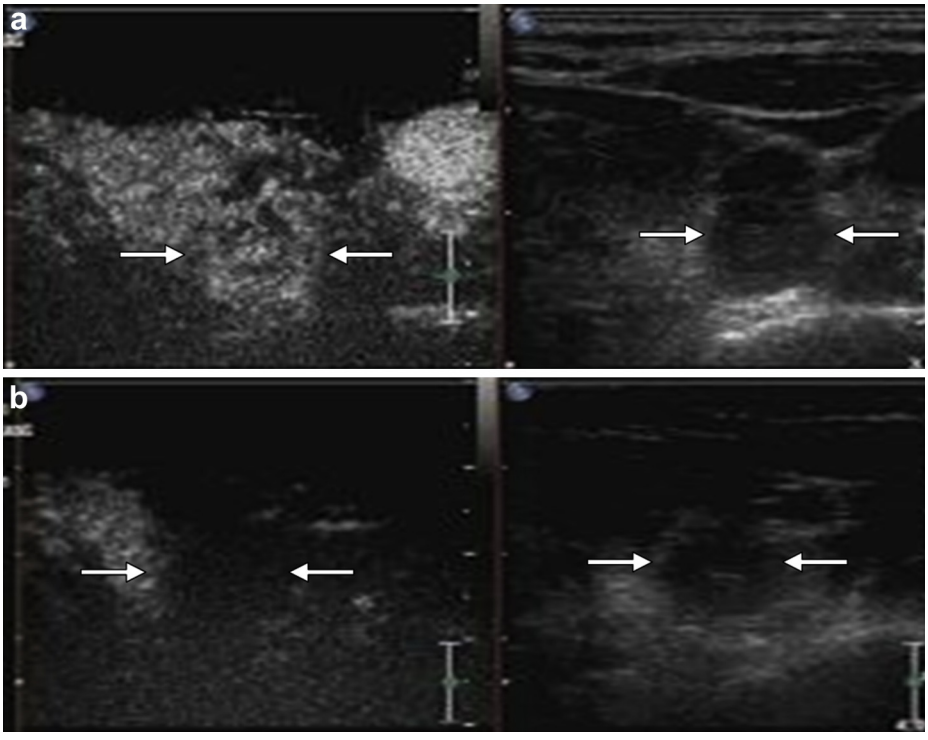

Fig. 4. A 48-y-old male with SHPT because of CRF for 6 y. (a) Contrast-enhanced ultrasound shows high enhancement of the enlarged parathyroideum before ablation (*arrow*) on left. B-mode ultrasound on right shows the same parathyroidhyperplasia on one picture. (b) Contrast-enhanced ultrasound shows no enhancement of the ablation zone in the procedure (*mark*) on the left. B-mode ultrasound shows the same parathyroid hyperplasia (*arrow*) on the right. SHPT = secondary hyperparathyroidism; CRF = chronic renal failure.

real-time dynamic images were stored in the ultrasound computer (Yuan et al. 2015). Patients were placed in the supine position with their necks fully exposed. Routine neck disinfection was performed and 2% lidocaine was used for topical anesthesia.

To protect the carotid artery, recurrent nerve and other adjacent structures, we devised a modified two-step procedure for ablation. The first step was intended to create a liquid isolation zone between parathyroid and adjacent structures. With a transverse guide and puncture targets appearing in the same ultrasound image on the transverse neck section as the needle and important anatomic structures, 5–20 mL of diluted 2% lidocaine was injected around the hyperplastic parathyroid to establish a buffer zone >1 cm wide between the gland and surrounding tissue (Fig. 2). The second step was the ablation itself. After forming a buffer zone, the ablation needle was inserted under ultrasound guidance into the parathyroideum (Fig. 3b), and ablation was performed for 3–5 s. Next, the probe was raised to move the already-ablated parathyroid toward the ventral side of the patient, away from the esophageal groove and toward the upper part of the trachea, to keep the buffer zone width >1 cm. The patient's voice was monitored during the operation, and the procedure was halted if dysphonia occurred. Ablation was performed and continued until the microbubbles generated by ablation filled the parathyroid gland completely. The Doppler sonication energy level or Manual Flash setting was used to burst the microbubbles. After ablation, CEUS was performed, and if there was no enhancement of the entire parathyroid gland (Fig. 4b), the procedure did not continue. sPTH was reviewed at 1 h and 1 wk after ablation. If sPTH decreased by <15% of its original level, a second ablation was performed.

Laboratory tests

sPTH, serum calcium and serum phosphorous were measured before the operation and at 1 h, 1 wk, 1 mo and 6 mo after treatment. Uremia patients with chronic renal failure could have abnormal serum calcium, phosphorus metabolic disorders and cause hyperparathyroidism. sPTH was measured by radiation immunoassay method (normal range 11–62 pg/mL). Serum calcium and serum phosphorous were measured by ethylenediamine tetraacetic acid (EDTA) titration method (normal range of serum calcium 2–2.5 mmol/L; normal range of serum phosphorous, 0.97–1.62 mmol/L). sPTH is the most important hormone regulating blood calcium and phosphorus levels, as it can increase the level of blood calcium and reduce levels of blood phosphorus. At the same time, the blood calcium and blood phosphorus levels also affect the secretion of sPTH: when serum Ca^{2+} increases, serum phosphorous is reduced and sPTH levels are downregulated; while serum Ca^{2+} is reduced, serum phosphorous increases and sPTH levels are upregulated.

Statistical analyses

Statistical analyses were performed using statistical software (SPSS for Windows version 17.0, SPSS Inc., Chicago, IL, USA). Continuous variables were expressed as the mean ± standard deviation and compared using paired *t*-tests. A p value < 0.05 was considered significant.

RESULTS

Ablations of 138 parathyroid glands were performed in 56 patients. All operations were performed in the outpatient clinic and each parathyroid was ablated for 5.24 ± 3.31 min. Fifty-six patients completed the 1-mo follow-up, and 34 patients completed the 6-mo follow-up visit.

The level of sPTH about 1 h after the operation decreased significantly compared with that before the operation ($p < 0.05$), and the level of sPTH 1 wk after the operation was significantly less than before the operation. It was not statistically different from that at 1 h after the operation, but there was a trend for sPTH to further decline by 1 wk. At 1 mo after the operation, sPTH trends increased compared with 1 wk after surgery, but the difference was not statistically significant ($p > 0.05$). The change in sPTH of all patients 1 mo after the operation indicated a significant short-term efficacy of the minimally invasive treatment for SHPT. The level of sPTH at 6 mo after the operation also decreased significantly compared with before operation in the 34 patients available for follow-up ($p < 0.05$; Table 1). No statistically significant changes were found for serum calcium or phosphorus at 1 h, 1 wk, 1 mo or 6 mo after treatment (Table 2). The improvement in bone pain was statistically significant ($p < 0.05$), although improvements in itchy skin and insomnia were not ($p > 0.05$; Table 3).

Two patients in this study, because of exceptional circumstances, were not included in the statistical

Table 1. Laboratory tests of sPTH before and after ablation

Time	N	sPTH (pg/mL)	*t*	*p*
Before ablation	54	1256.4 ± 461.0		
1 h after ablation	54	438.7 ± 191.8	17.838	<0.001
1 w after ablation	54	408.8 ± 194.2	17.728	<0.001
1 m after ablation	54	446.7 ± 186.6	17.421	<0.001
6 m after ablation	34	442.4 ± 234.6	13.098	<0.001

sPTH = serum parathyroid hormone.

Table 2. Laboratory tests of serum calcium and phosphorous before and after ablation

Time	N	Serum calcium (mmol/L)	*t*	*p*	Serum phosphorous (mmol/L)	*t*	*p*
Before ablation	54	2.25 ± 0.29			1.47 ± 0.48		
1 h after ablation	54	2.20 ± 0.25	1.101	0.276	1.59 ± 0.93	1.409	0.165
1 w after ablation	54	2.29 ± 0.23	1.042	0.302	1.55 ± 0.48	0.98	0.331
1 m after ablation	54	2.25 ± 0.20	0.122	0.904	1.44 ± 0.41	0.418	0.677
6 m after ablation	34	2.25 ± 0.28	0.256	0.800	1.35 ± 0.34	1.696	0.099

analysis. In these two patients, four hyperplastic parathyroids were found in the neck by ultrasound and radionuclide imaging. The level of sPTH initially decreased significantly, but then became re-elevated to the original levels by 1 wk post-treatment. One patient had radionuclide imaging performed again, and one parathyroid hyperplasia was found behind the sternum; the other patient refused any additional testing.

In this study, two cases had temporary hoarseness after operation but recovered without treatment within 1 wk. One case developed permanent hoarseness (laryngoscopy showed the homonymy vocal cord was paralyzed) and was given neurotropic medicine, with gradual improved by 4 mo post-treatment.

DISCUSSION

The results of our study were consistent with those of other studies (Wang et al. 2011; Zhang et al. 2013b) and proved that the ablation technique can rapidly destroy tumor tissue. sPTH was significantly reduced post-operatively and some symptoms also improved for patients, especially bone pain. However, itching and insomnia showed only statistically insignificant trends of improvement. This could be a result of elevated sPTH causing high blood phosphorus and low blood calcium—itchiness is a neurotoxic effect caused by calcium salt deposition—but it could also be caused by a number of other things such as nitrogen metabolites or cutaneous stimulation. Patients with renal failure frequently experience allergic skin reactions, and tolerance for symptoms varies between patients.

The technique fails to reach the same effect as complete tumor resection, but the symptoms of patients were mitigated, especially regarding bone pain, which was eliminated in six patients. Through the post-operative follow-up, it was observed that patients' sPTH rebounded slightly after 1 mo. This could be explained in several ways. First, the body and sPTH levels may go through an adjustment period after treatment. Second, to ensure that no damage was caused to important anatomic structures (including the thyroid, carotid artery, esophagus, trachea and recurrent laryngeal nerve), edges of tumors were not completely ablated. Third, based on available experimental and clinical data, we have come to the conclusion that it is necessary to maintain a temperature of 54°C for no less than 1 min or a temperature of 60°C to achieve irreversible tissue coagulation (Godlewski et al. 1988). The mean temperature at the site 5 mm from the electrode was driven rapidly to 60°C, which ensured tumor necrosis, whereas the maximum temperatures at 10 and 15 mm were lower (Feng et al. 2012), which would guarantee the safety of surrounding tissue but could leave residual tumor cells that could resume function after some time. The sPTH 1 mo after treatment did tend to increase. This technique is relatively less invasive compared with surgery and did not cause refractory hypocalcemia in this experiment. In the study, monitoring of serum calcium and phosphorous was necessary to detect potentially low serum calcium after ablation.

Two exceptional cases in this study had different sPTH outcomes after the treatment. In both patients, the parathyroid showed no enhancement on ultrasound or radionuclide images. We first considered the possibility of ectopic parathyroid hyperplasia, which was true with one. This highlights that a limitation of this technology is the requirement for precise localization of nodules and instrumentation. Three patients developed hoarse voices, which could be caused by rapid fluid loss, lack of isolation width, temporary paralysis of the laryngeal

Table 3. Symptom scores of bone pain, itching and insomnia before and after ablation

Time	Bone pain	N	*t*	*p*	Itching	N	*t*	*p*	Insomnia	N	*t*	*p*
Before ablation	6.61 ± 2.02	38			7.38 ± 1.53	21			14.14 ± 2.21	14		
1 h after ablation	2.00 ± 1.19	38	1.460	0.028	2.33 ± 1.15	21	0.848	0.469	2.93 ± 0.73	14	0.948	0.330
1 w after ablation	1.84 ± 1.03	38	1.999	0.001	2.05 ± 0.87	21	1.318	0.062	3.14 ± 0.95	14	0.918	0.369
1 m after ablation	2.00 ± 1.01	38	2.109	<0.01	2.38 ± 0.87	21	1.326	0.059	3.36 ± 0.75	14	1.224	0.100
6 m after ablation	1.88 ± 1.01	32	2.047	<0.01	2.69 ± 0.60	16	1.293	0.071	3.167 ± 0.72	12	0.895	0.399

recurrent nerve or other factors. Injected liquid would easily flow into the surrounding tissue and the puncture squeeze will accelerate the loss of liquid, reducing or eliminating the isolation area. Supplying liquid to maintain the buffer zone also had some limitations as it increased the difficulty, complexity and risk of the operation. Abnormalities of the recurrent laryngeal nerve are also possible (Fellmer et al. 2008; Lee et al. 2009). Because the inner diameter of the recurrent laryngeal nerve is about 1 mm and a L12-5 transducer operating at a frequency between 5 and 12 MHz can not visualize it, it is difficult to find the position of the recurrent laryngeal nerve and avoid it during ablation. Two of cases of temporary hoarseness were possibly caused by lidocaine. The patient suffering from permanent hoarseness had significant parathyroid hyperplasia, with a longitudinal diameter of 3.2 cm and transverse diameter of 2.6 cm. Although a buffer zone was established and the gland moved, the separation effect may not be obvious and the recurrent laryngeal nerve could have been subjected to a certain amount of heat injury.

Parathyroids are located in the neck's "dangerous triangle," adjacent to the recurrent laryngeal nerve and neck blood vessels. This location has the most complicated relationship with the recurrent laryngeal nerve. Without precautions, ablation might lead to irreversible damage. Therefore, taking certain precautions to protect the recurrent laryngeal nerve plays a critical role in the operation and the process of protecting adjacent tissue is the novel aspect of our work. In this study, we built a buffer zone that separated the gland and surrounding tissue.

During the procedure, we lift the parathyroid up and away from the esophagus, tracheal groove and surrounding tissue. This increased the distance between the ablation needle and sensitive surrounding tissue to minimize complications. This technique is not widely used to prevent damage from thermal ablation therapy, as there is only one report of similar method in the treatment of renal tumors in radiofrequency ablation (Boss et al. 2005). In that study, the researchers raised the radiofrequency needle to pull the kidney away from surrounding tissue and avoided thermal damage to the surrounding tissue. However, the parathyroid hyperplasia is softer in texture, so if we were to immediately lift the ablation pin after pushing it into the nodule, it would not raise the nodule. We found we could ablate glands for 3–5 s and when the surrounding tissue becomes dehydrated, coagulated and hardened, it could be lifted to increase the safety distance and avoid thermal damage. The study had found that the incidence of voice hoarseness was 5%, significantly lower than the study of Zhang et al. (2013a), which was 66.7%.

SPTH recurrence after ablation has not been determined in this study, but we will continue to conduct follow-up observation for the long-term effects.

CONCLUSION

In conclusion, ultrasound-guided percutaneous ablation therapy of SHPT is a newly emerging technology that is minimally invasive and highly targetable, requires shorter ablation time and is associated with little pain. Patients do not require hospitalization and have fewer complications, and treatment can be repeated. However, the efficacy and tolerability of ultrasound-guided ablation of SHPT needs further evaluation. In the future, this technology may be a preferred method for treatment of SHPT.

Acknowledgments—This study was funded by Capital characteristic clinical application research in 2013 (Z131107002213143).

REFERENCES

Bennedbaek FN, Karstrup S, Hegedüs L. Ultrasound guided laser ablation of a parathyroid adenoma. Br J Radiol 2001;74:905–907.

Bolasco P. Effects of the use of non-calcium phosphate binders in the control and outcome of vascular calcifications: A review of clinical trials on CKD patients. Int J Nephrol 2011;2011:758450.

Bornivelli C, Alivanis P, Giannikouris I, Arvanitis A, Choustoulakis I, Georgopoulou K, Karvouniaris N, Zervos A. Relation between insomnia mood disorders and clinical and biochemical parameters in patients undergoing chronic hemodialysis. J Nephrol 2008; 21(Suppl 13):S78–S83.

Boss A, Clasen S, Kuczyk M, Anastasiadis A, Schmidt D, Claussen CD, Schick F, Pereira PL. Thermal damage of the genitofemoral nerve due to radiofrequency ablation of renal cell carcinoma: A potentially avoidable complication. Am J Roentgenol 2005;185:1627–1631.

Chen HH, Lin CJ, Wu CJ, Lai CT, Lin J, Cheng SP, Yang TL. Chemical ablation of recurrent and persistent secondary hyperparathyroidism after subtotal parathyroidectomy. Ann Surg 2011;253:786–790.

Douthat WG, Garay G, de Arteaga J, Fernández Martin JL, Cannata Andia JB, Massari PU. Biochemical and histological spectrum of renal osteodystrophy in Argentina. Nefrologia 2003;23:47–51.

Douthat WG, Cardozo G, Garay G, Orozco S, Chiurchiu C, de la Fuente J, de Arteaqa J, Massari PU. Use of percutaneous ethanol injection therapy for recurrent secondary hyperparathyroidism after subtotal parathyroidectomy. Int J Nephrol 2011;2011:246734.

Fellmer PT, Böhner H, Wolf A, Röher HD, Goretzki PE. A left nonrecurrent inferior laryngeal nerve in a patient with fight-sided aorta, truncus arteriosus communis, and an aberrant left innominate artery. Thyroid 2008;18:647–649.

Feng B, Liang P, Cheng Z, Yu X, Yu J, Han Z, Liu F. Ultrasound-guided percutaneous microwave ablation of benign thyroid nodules: Experimental and clinical studies. Eur J Endocrinol 2012;166: 1031–1037.

Godlewski G, Rouy S, Pignodel C, Ould-Said H, Eledjam JJ, Bourgeois JM, Sambuc P. Deep localized neodymium (Nd)-YAG laser photocoagulation in liver using a new water cooled and echo-guided handpiece. Lasers Surg Med 1988;8:501–509.

Hänsler J, Harsch IA, Strobel D, Hahn EG, Becker D. Treatment of a solitary adenoma of the parathyroid gland with ultrasound-guided percutaneous Radio-Frequency-Tissue-Ablation (RFTA). Ultraschall Med 2002;23:202–206.

Hensley CP, Courtney CA. Management of a patient with chronic low back pain and multiple health conditions using a pain mechanisms-based classification approach. J Orthop Sports Phys Ther 2014;44:403.

Keithi-Reddy SR, Patel TV, Armstrong AW, Singh AK. Uremic pruritus. Kindey Int 2007;72:373–377.

Lacobone M. Is ultrasound-guided laser thermal ablation for parathyroid adenomas safe and effective? Horm Res 2006;66:94–95.

Lee MS, Lee UY, Lee JH, Han SH. Relative direction and position of recurrent laryngeal nerve for anatomical configuration. Surg Radiol Anat 2009;31:649–655.

Lencioni RA, Allgaier HP, Cioni D, Olschewski M, Deibert P, Crocetti L, Frings H, Laubenberger J, Zuber I, Blum HE, Bartolozzi C. Small hepatocellular carcinoma in cirrhosis: Randomized comparison of radio-frequency thermal ablation versus percutaneous ethanol injection. Radiology 2003;228:235–240.

Liang P, Dong B, Yu X, Yu D, Cheng Z, Su L, Peng J, Nan Q, Wang H. Computer-aided dynamic simulation of microwave-induced thermal distribution in coagulation of liver cancer. IEEE Trans Biomed Eng 2001;48:821–829.

Lin SM, Lin CJ, Lin CC, Hsu CW, Chen YC. Radiofrequency ablation improves prognosis compared with ethanol injection for hepatocellular carcinoma ≤4 cm. Gastroenterology 2004;127:1714–1723.

Liu Y, Zhang JH, Gao XB, Wu XJ, Yu J, Chen JF, Bian SZ, Ding XH, Huang L. Correlation between blood pressure changes and AMS, sleeping quality and exercise upon high-altitude exposure in young Chinese men. Mil Med Res 2014;26:1–19.

Lu MD, Xu HX, Xie XY, Yin XY, Chen JW, Kuang M, Xu ZF, Liu GJ, Zheng YL. Percutaneous microwave and radiofrequency ablation for hepatocellular carcinoma: A retrospective comparative study. J Gastroenterol 2005;40:1054–1060.

Moe S, Drüeke T, Cunningham J, Goodman W, Martin K, Olgaard K, Ott S, Sprague S, Lameire N, Eknoyan G. Kidney Disease: Improving Global Outcomes (KDIGO): Definition, evaluation, and classification of renal osteodystrophy: A position statement from Kidney Disease: Improving Global Outcomes (KDIGO). Kidney Int 2006;69:1945–1953.

Morrone LF, Russo D, Di lorio B. Diagnostic workup for disorders of bone and mineral metabolism in patients with chronic kidney disease in the era of KDIGO Guidelines. Int J Nephrol 2011;2011:958798.

Olson JA Jr, Leight GS Jr. Surgical management of secondary hyperparathyroidism. Adv Ren Replace Ther 2002;9:209–218.

Panichi V, Bigazzi R, Paoletti S, Mantuano E, Beati S, Marchetti V, Bernabini G, Grazi G, Giust R, Rosati A, Migliori M, Pasquariello A, Panicucci E, Barsotti G, Bellasi A. Impact of calcium, phosphate, PTH abnormalities and management on mortality in hemodialysis: Results from the RISCAVID study. J Nephrol 2010; 23:556–562.

Shibata T, Limuro Y, Yamamoto Y, Maetani Y, Ametani F, Itoh K, Konishi J. Small hepatocellular carcinoma: Comparison of radiofrequency ablation and percutaneous microwave coagulation therapy. Radiology 2002;223:331–337.

Shiina S, Teratani T, Obi S, Sato S, Tateishi R, Fujishima T, Ishikawa T, Koike Y, Yoshida H, Kawabe T, Omata M. A randomized controlled trial of radiofrequency ablation with ethanol injection for small hepatocellular carcinoma. Gastroenterology 2005;129:122–130.

Tungjitkusolmun S, Staelin ST, Haemmerich D, Tsai JZ, Webster JG, Lee FT Jr, Mzhvi DM, Vorperian VR. Three-dimensional finite-element analyses for radio-frequency hepatic tumor ablation. IEEE Trans Biomed Eng 2002;49:3–9.

Wang J, Han F, Zhao Q, Chen F, Zhang P, Huang H, Wang R, Jiang T, Chen J. Three cases of secondary and tertiary hyperparathyroidism treated with radiofrequency ablation. Chinese Journal of Nephrology 2011;27:712.

Yao L, Zhang L, Liu P, Bian W, Hua Z, Zhang J, Li W, Chen Y. Therapeutic evaluation of parathyroidectomy for 89 cases with refractory secondary hyperparathyroid-ism. Chinese Journal of Blood Purification 2009;8:431–436.

Young EW, Akiba T, Albert JM, McCarthy JT, Kerr PG, Mendelssohn DC, Jadoul M. Magnitude and impact of abnormal mineral metabolism in hemodialysis patients in the Dialysis Outcomes and Practice Patterns Study (DOPPS). Am J Kidney Dis 2004;44:34–38.

Yuan Z, Quan J, Yunxiao Z, Jian C, Zhu H. Contrast-enhanced ultrasound in the diagnosis of solitary thyroid nodules. J Cancer Res Ther 2015;11:41–45.

Zhang J, Qiu M, Sheng J,Lu F, Zhao L, Zhang H, Diao Z. Ultrasound-guided percutaneous thermal ablation for benign parathyroid nodules. Academic Journal of Second Military Medical University 2013a;34:362–370.

Zhang Z, Wang Q, Liu Y. Different treatments for secondary hyperparathyroidism of end-stage renal disease. International Medicine and Health Guidance News 2013b;19:3322–3325.